Research Article **ISSN: 2395 – 5597**

International Journal of Engineering and Robot Technology

Journal home page: www.ijerobot.com

https://doi.org/10.36673/IJEROBOT.2020.v07.i02.A07

CFD ANALYSIS OF FLOW IN WINDOWLESS ACCELERATED DRIVEN SUB-CRITICAL (ADS) REACTOR TARGET MODULE

A. P Senthil Kumar*[1], Sayed Mohammed Saud[1], S. Janaki[2], M. Muthukumar[3]

[1*]Department of Mechanical Engineering, PSG College of Technology, Coimbatore, Tamil Nadu, India.
[2]Department of Mechatronics Engineering, SNS Collge of Technology, Coimbatore, Tamil Nadu, India.
[3]Department of Mechanical Engineering, Nandha Engineering College, Erode, Tamil Nadu, India.

ABSTRACT

The Spallation target is the most critical part of an Accelerated Driven Sub-Critical (ADS) reactor system. In this paper a numerical study of fluid flow and heat transfer for two possible types of windowless spallation targets was done with finite volume CFD code Fluent. In the first target module, Lead-Bismuth Eutectic (LBE) falling downwards through annular nozzle and forming a free surface is simulated using two phase mixture model with cavitation mass transfer to obtain the interface. Second target with LBE flowing upwards horizontally in an inverted-U fashion is simulated starting with a basic sharp design and later including modifications to improve the flow and eliminate recirculation zones. Spallation heat was simulation and temperature profile revealed steady convection without heat accumulation.

KEYWORDS

ADS, Spallation target, Lead-bismuth eutectic, Thermal-hydraulics and VOF.

Author for Correspondence:

Senthil Kumar A P,

Department of Mechanical Engineering,

PSG College of Technology,

Coimbatore, Tamil Nadu, India.

Email: apspsgct@yahoo.com

INTRODUCTION

The Accelerated Driven Sub-Critical system is a promising type of reactor system that have dual purpose of nuclear waste incineration (Transmutation)[1] and energy generation from lower grade fuel like Thorium. The most critical part of this system is the target which contains heavy liquid metal (HLM) such as Lead-Bismuth Eutectic (LBE) on which high energy protons impinge to produce neutrons by spallation. The subcritical core relies on these spallation neutrons to sustain fission. Thus the HLM is the target for spallation as well as coolant to

carry away the generated spallation heat. Initial target designs contained a physical window at the end of the beam tube, but material limitations have forced to look towards alternative designs without a window. A lot of studies have been carried out on window target. Arul Prakash K[2] performed thermal hydraulic study with streamline Petrov upwind galerkin based FEM code. Cho *et al*[3]. Obtained the optimal design parameters of a 20MW spallation target for a 1000MWth ADS.

Unlike in window target where the flow is single phase and stable, the flow in windowless target is multiphase with an unstable interface on which the beam will act. Thus, it is a challenging task to study this two phase HLM-vacuum interface. Roelofs *et al*[4]. Reviewed the development of ADS windowless spallation target in the experiment and the numerical simulation. Most common design of windowless target is the MYRRHA[5] ADS target developed by Belgian nuclear agency SCKCEN within the EUROTRANS project. Numerical simulation campaigns on MYRRHA by Batta and Class[6], Su *et al*[7], J. Liu *et al*[8]. Have been supported by experimental results obtained on water loop by Xiong[9] and HLM loops by Jeanmart[10] and Liftin *et al*[11].

In this study two possible windowless target designs are studied, one with LBE falling down through an annular nozzle (i.e. MYRRHA ADS target[6]) and another with flow in inverted-U turn fashion like in XDS[12].

MYRRHA LBE SIMULATION

Geometry

During EUROTRANS the design of the windowless target has been evolved to the design (V0.10)[6]. The overall dimension is 196.96mm x 725.1mm and the size of the vacuum tube is 91.7mm x 305.13mm. The main objective of the ADS target is to have a stable free surface with less recirculation.

Numerical model

Batta and Class[6] found that volume of fluid (VOF) method[13] combined with cavitation model is an ideal numerical model to track the free surface LBE-vacuum interface. But in Fluent cavitation models cannot be used with the VOF model because the surface tracking schemes for the VOF model are incompatible with the interpenetrating continua assumption of the cavitation models, so instead a mixture model was used. Mixture model is inherently similar to VOF model but differs in the aspect that it considers the phases to be interpenetrating and allows slip velocity between them. It also enables mass, momentum and energy transfer between phases. Here vacuum was modelled as imaginary LBE-vapor and proton tube outlet was assigned boundary condition pressure lower than the LBE vapor pressure at the operating temperature. So, when liquid LBE is in this lower pressure region, cavitation and hence mass transfer will occur from liquid to vapor and would hence generate an interface. It is important to note that there is no real cavitation in the target but is used to simulate vacuum as an incompressible light fluid in the VOF-context and creates/eliminates vacuum wherever appropriate. Cavitation source terms for the growth/ collapse of vapor bubbles is modelled by the Schnerr and Sauer model[14].

Governing Equations

The flow is governed by the flowing set of conservation equations. The continuity equation is given as:

$$\frac{d(\rho_m)}{dt} + \nabla.(\rho_m \vec{v}_m) = \dot{m} \qquad (1)$$

Where $\dot{m}$ is the mass transfer due to cavitation, ρ_m is the mixture density and $\vec{v}_m$ is the mass-averaged velocity, both given below as:

$$\rho_m = \alpha_l \rho_l + \alpha_v \rho_v \qquad (2)$$

$$\vec{v}_m = \frac{\alpha_l \rho_l \vec{v}_l + \alpha_v \rho_v \vec{v}_v}{\rho_m} \qquad (3)$$

Here α is the volume fraction and the subscript l refers to LBE liquid and v refers to LBE vapor. From the continuity equation for secondary phase, the volume fraction equation for secondary phase, α_v can be obtained

$$\frac{d(\alpha_v \rho_v)}{dt} + \nabla.(\alpha_v \rho_v \overrightarrow{v_m}) = -\nabla.\left(\alpha_v \rho_v \vec{v}_{dr,v}\right) + \sum_{g=1}^{n} (m_{lv} - m_{vl}) \quad (4)$$

Here m_{lv} and m_{vl} are the mass transfer source terms from liquid to vapor and vice-versa. The momentum equation is given as:

$$\frac{d(\rho_m \vec{v}_m)}{dt} + \nabla.(\rho \vec{v}_m \vec{v}_m) = -\nabla.p + \nabla.\left[\mu_m\left(\nabla \vec{v}_m + \nabla \vec{v}_m{}^T\right)\right] + \rho_m \vec{g} + \vec{F} + \nabla.\left(\alpha_v \rho_v \vec{v}_{dr,v} \vec{v}_{dr,v}\right) \quad (5)$$

Where, μ_m is the mixture viscosity and $\vec{v}_{dr,k}$ is the drift velocity for secondary phase both given respectively as:

$$\mu_m = \alpha_l \mu_l + \alpha_v \mu_v \quad (6)$$

$$\vec{v}_{dr,v} = \vec{v}_v - \vec{v}_m \quad (7)$$

Mesh

The 2-D symmetrical structed mesh with quadrilateral face elements and grading at crucial sections like nozzle flow detachment was adopted. A mesh sensitivity study was done to determine the mesh independency. Also, as most of the turbulent eddies are dissipated in the Taylor micro scale range, which is based on maximum Reynolds number (7×10^4) and integral length scale (100mm) and found to be 1.46mm.

$$\lambda = L\left(\frac{15}{Re}\right)^{0.5} \quad (8)$$

Properties, Boundary conditions and Solution method

The temperature dependent thermo-physical properties of LBE liquid by Sobolev[15] were evaluated at the operating temperature of 723 K. For vapor however properties were approximated with those of pure lead vapor.

Symmetric boundary condition for the axis and no slip boundary condition for the walls of the target module was assigned. The beam tube opening is assigned the pressure outlet boundary condition with pressure lower than the LBE vapor pressure so that cavitation is initiated. Turbulence is modelled by standard κ-ϵ turbulence model. Transient simulation is run until steady state is reached with variable time step to keep the global courant number below 1 for better convergence. PISO solution algorithm is used for pressure-velocity coupling. PRESTO scheme is used to discretise Pressure field, while second order upwind scheme is used for rest parameters for their better accuracy and transportivness. Convergence criteria for continuity, velocity components, turbulent kinetic energy and specific dissipation energy is set to 10^{-6}.

Result

As the simulation progresses, the pressure fields get adjusted and when the total pressure is lower than the LBE vapor pressure, cavitation mass transfer occurs. This automatically adjust the interface accordingly till a steady state is reached. It was seen that the interface profile depends on the inlet velocity and outlet pressure as anticipated.

INVERTED-U TARGET SIMULATION

Geometry

In the second windowless target design, the LBE flows horizontally with respect to the beam at the spallation region as shown in Figure No.4. LBE is pumped upwards near the target where it moves horizontally for a moment before plunging downwards due to gravity. The objective is to have a stable fluid-vacuum interface at the windowless section. Also, the residence time of fluid inside the target should be low without recirculation zones and the horizontal component of velocity must be large enough near the spallation region to advect the generated heat.

Volume of Fluid (VOF) Method

VOF method tracks the interface by calculating the volume fraction in each cell and constructing it with suitable scheme. The flow is isothermal, turbulent and multiphase with free surface. The effect of gravity, implicit body forces and surface tension between phases is included. The conservation equation for VOF method are given below with phase continuity equation as:

$$\frac{\partial \alpha_w}{\partial t} + \vec{v}_w.\nabla \alpha_w = 0 \quad (9)$$

$$\frac{\partial \alpha_a}{\partial t} + \vec{v}_a.\nabla \alpha_a = 0 \quad (10)$$

Where $\vec{v}_w$ and $\vec{v}_a$ are the velocity vectors and α_w and α_a are the volume fractions of water and air respectively and are governed by an additional constraint:

$$\alpha_w + \alpha_a = 1 \quad (11)$$

The properties such as density and viscosity for cells with interface are calculated as the mixture of both the phases

$$\mu = \alpha_a \mu_a + (1 - \alpha_a)\mu_w \quad (12)$$

$$\rho = \alpha_a \rho_a + (1 - \alpha_a)\rho_w \quad (13)$$

The VOF Momentum is solved by fluent as

$$\frac{\partial(\rho\vec{v})}{\partial t} + \nabla.(\rho\vec{v}\vec{v}) = -\nabla.p + \nabla.[\mu(\nabla\vec{v} + \nabla\vec{v}^T)] + \rho\vec{g} + \overrightarrow{f_{sv}} \quad (14)$$

Where $\vec{v}$ is the velocity vector of mixed fluid, p is the static pressure, $\rho\vec{g}$ is the gravitational body force and $\overrightarrow{f_{sv}}$ is the surface tension force which is given by Continuum surface force model (CSF)[16], which transforms a surface tension force to a volumetric force by:

$$\vec{f}_{sv} = 2\sigma \frac{\rho\nabla\alpha_w}{r(\rho_w + \rho_a)} \quad (15)$$

Here σ is the surface tension coefficient between the phases ($\sigma = 0.072\ N/m$) and r is the liquid-gas interface radius calculated from:

$$\frac{1}{} = \nabla.\frac{\nabla}{|\nabla\ |} \quad (16)$$

Boundary conditions and solution methods

A 2D computational domain of the test section (Figure) is discretized with a structed mesh. The mesh is made of quadrilateral elements with mean size of 5mm which conforms to grid independency. The interface is tracked with geo-reconstruct scheme which is Fluent equivalent of Piecewise Linear Implicit calculation (PLIC)[17]. PISO algorithm has been adopted for velocity-pressure coupling. The discretization schemes and convergence criteria are same as previous simulation. The solution is initialized from inlet with water phase in the whole domain.

The transient simulation showed that a stable interface is attained in short time (up to 10 sec) after some initial fluctuations. The flow fields and streamline showed the presence of a large vortex at the top left corner of the target and another at the bottom of spallation zone due to sharp abrupt turns. The horizontal component of velocity is very low near the interface. The low velocities and the recirculating region constitute the main drawback and it is necessary to modify the target geometry.

Design improvements

In order to obtain a more suitable flow field the target corners are rounded with a suitable profile to eliminate the large vortex. But inspite of rounded edges it was seen that the recirculation zone at the bottom was present and the velocity at upper spallation region was nearly zero. To solve this problem the idea of inclusion of internal guides vanes was tested. Guide vanes drive the flow together uniformly at the spallation region and hence reduce the bottom recirculation zone. A numerical study has been performed to evaluate the effect of these modifications. The number of guide vanes are varied to study the velocity and pressure drop.

In order to obtain a more suitable flow field the target corners are rounded with a suitable profile to eliminate the large vortex. But inspite of rounded edges it was seen that the recirculation zone at the bottom was present and the velocity at upper spallation region was nearly zero. To solve this problem the idea of inclusion of internal guides vanes was tested. Guide vanes drive the flow together uniformly at the spallation region and hence reduce the bottom recirculation zone. A numerical study has been performed to evaluate the effect of these modifications. The number of guide vanes are varied to study the velocity and pressure drop.

It was seen that introduction of guide vanes produces higher velocities at the interface while smooth corners prevent the occurrence of recirculating regions. The vanes guide the flow neatly resulting in uni-directional streamlines with no recirculation in the flow domain. But the velocity is not uniform at the spallation region but is sinusoidal due to wakes created by inclusion of vanes. The non -uniform velocity profile and the increased pressure drop due to vanes are some of the drawbacks.

Thermal simulation

Spallation heat distribution for window target is generally obtained from monte Carlo based nuclear transport codes like FLUKA, LAHAT[18] etc. but are difficult to access. An alternative strategy is to introduce constant heat flux planer source at steady state interface region in the domain itself.

The heat generated is highest at the interface and decreases downwards as the beam penetrates. Therefore, a triangular shaped source for 2D geometry with maximum value at top and zero at bottom is considered. The top edge length of the triangle will be equal to the beam diameter i.e. 100mm and its depth will be equal to depth of beam

penetration (470mm). The beam power dissipated as heat is 1MW and the heat source value in terms of heat flux per unit volume equals 800MW/m^3. This is modelled in the cell zone condition of the spallation source region. This adds the heat source term in the energy equation in those particular cells. The velocity fields already obtained are then coupled to this source and steady state temperature profile of the target is obtained.

Thermal simulation for target with vanes showed that the generated heat is effectively carried away by the fluid. The temperature profile at source resembles wavy nature due to the effect of separation of flow from the vanes.

Table No.1: Grid sensitivity study at coordinates (0.041, -0.23)

Mesh elements	8696	13649	18241	24233
Velocity (m/s)	2.069	2.215	2.207	2.206
Static pressure(Pa)	2376.33	2384.59	2387.41	2388.09

Table No.2: Properties of LBE Liquid and Vapor

S.No	**Property**	**Equation**	**Value (SI)**
1	Density of liquid, ρ_l	$11{,}096 - 1.3236 \times T$	10139
2	Viscosity of liquid, μ_l	$4.94 \times 10^{-4} \times e^{754.1/T}$	1.4 x 10^{-3}
3	Saturated pressure	$1.11 \times 10^{10} \times e^{-22{,}552/T}$	2370
4	Density of vapor, ρ_v	$-1.939 + 0.00149 \times T$	0.2215
5	Viscosity of vapor, μ_v	$14.43T^{0.5}/(0.003T^{-0.15} + 8.5e^{-1.4\times10^{-4}T})$	5.32 x 10^{-5}

Table No.3: Numerical model and boundary condition

Multiphase model	Mixture model with slip velocity between phases.
Primary/ secondary phase	LBE-liquid / LBE-vapor
Phase interaction	Cavitation mass transfer, Schnerr and Sauer model
Cavitation pressure	2370 Pa
Inlet	Velocity inlet, 0.8 m/s
Outlet	Pressure outlet 22000 Pa-35000 Pa
Outlet 2:	Pressure outlet 2330 Pa (<2370 Pa)
Operating pressure / density	0 Pa (vacuum) / 0.2215 kg/m^3
Initialization	Standard; from inlet, with liquid in whole domain

Table No.4: Result of numerical study by varying vanes

S.No	**No. of vanes**	**Pressure drop across vanes (ΔP) Pa**	**Max. Temp. Rise (ΔT_{max}) K**	**Spallation section Avg. vel. (V_{avg}) m/s**
1	0	__	216	0.415
2	3	386.3	35.3	0.587
3	4	450.4	27	0.628
4	5	508.8	24	0.684

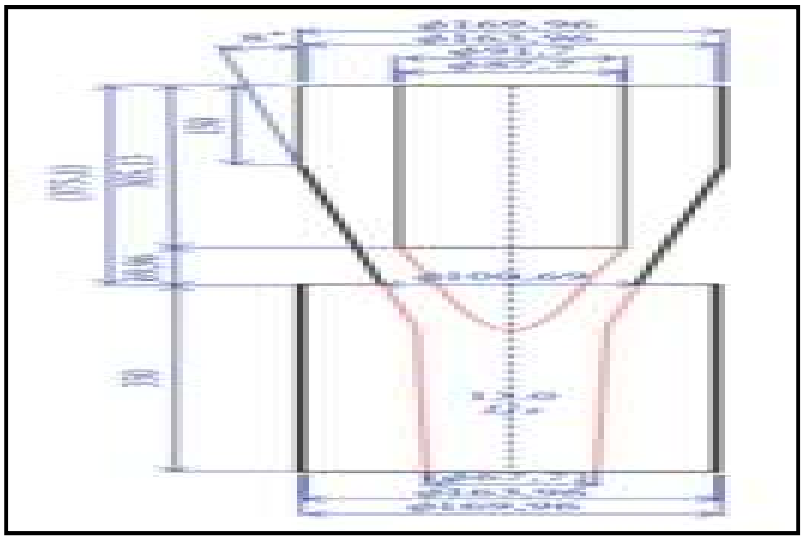

Figure No.1: Schematic diagram of MYRRHA Spallation target module[6]

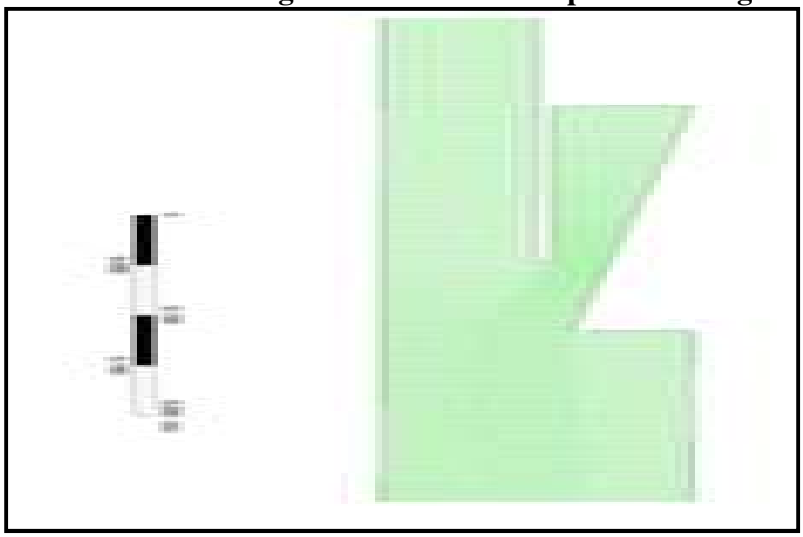

Figure No.2: 2-D symmetrical domain with meshing

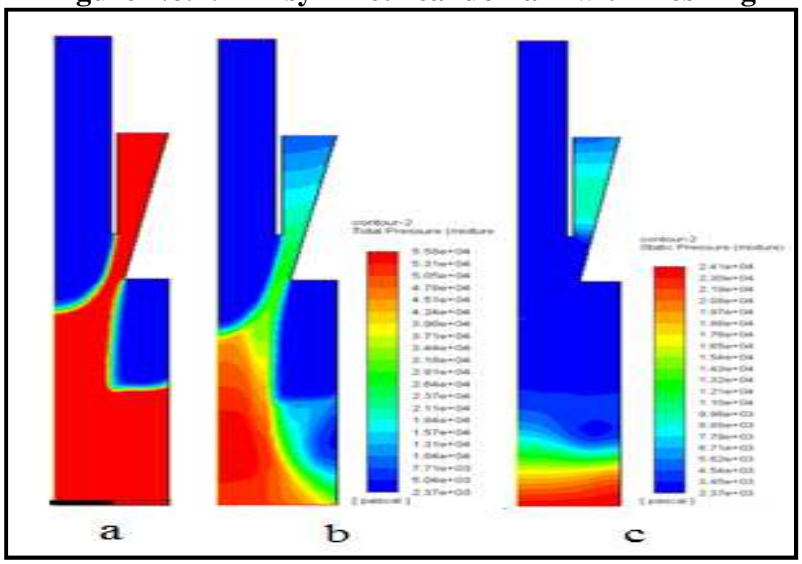

Figure No.3: (a) Volume fraction {red: LBE liquid; blue: vapor} (b) Total pressure (c) static pressure

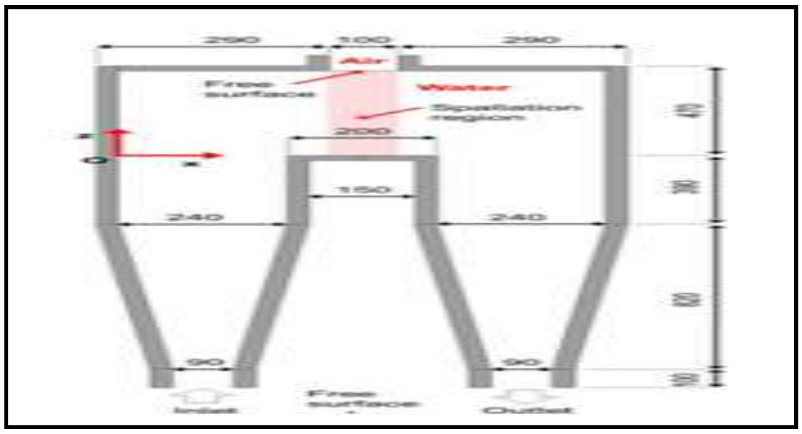

Figure No.4: Schematic diagram of Inverted-U

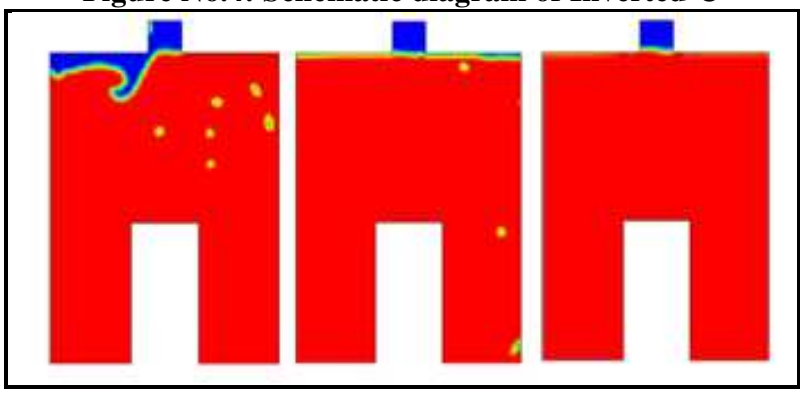

Figure No.5: Transient VOF volume fraction contours in inverted-U target (red: water, blue: air). The interface is stable after some fluctuations on initiating the flow form inlet

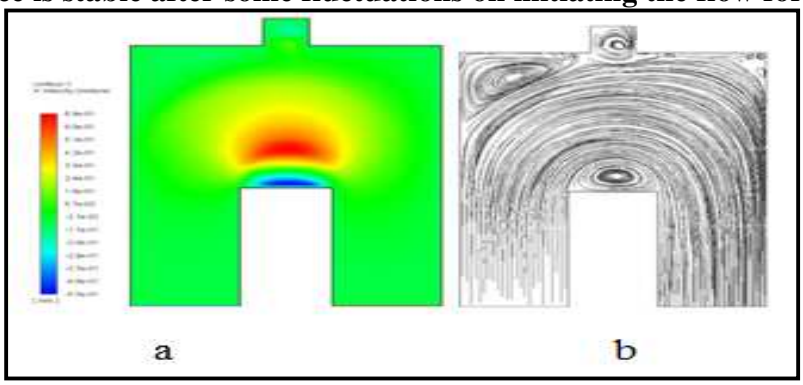

Figure No.6: (a) x-velocity component and (b) pathlines of flow in basic inverted-U target

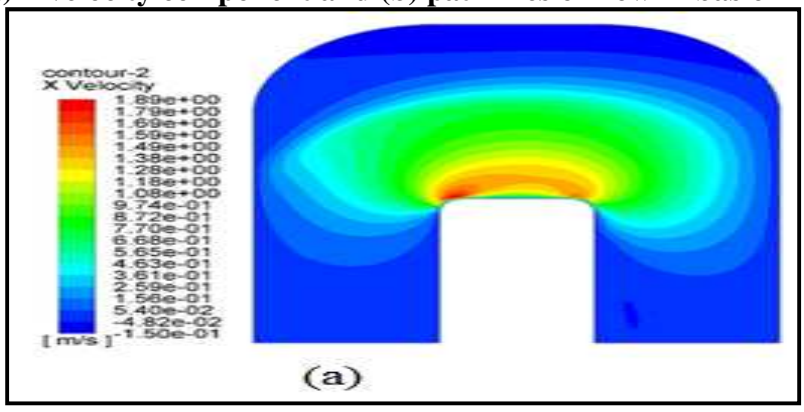

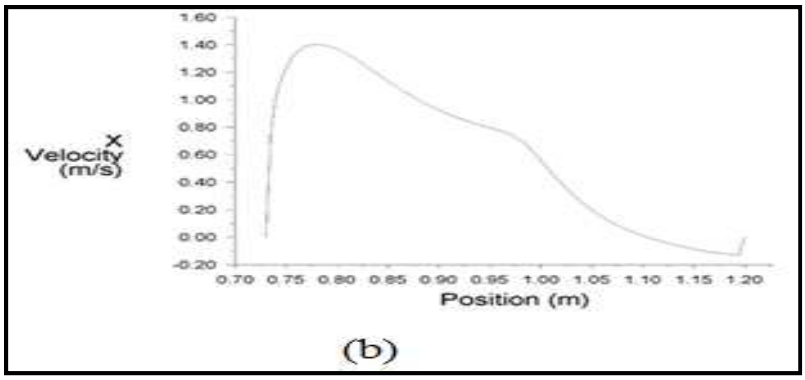

Figure No.7: (a) Horizontal x-velocity contours in modified inverted-U target with rounded edges (b) velocity profile against Z-axis at spallation region. The velocity at should be high at the end of the X-axis

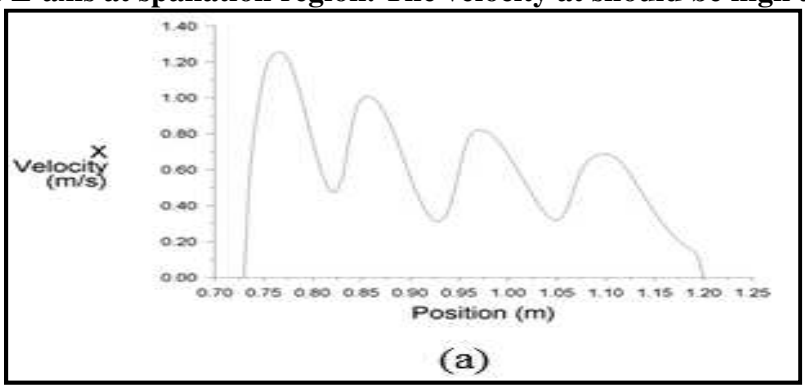

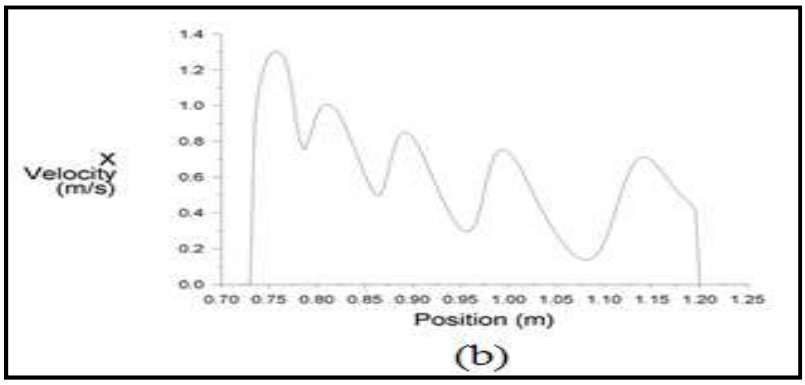

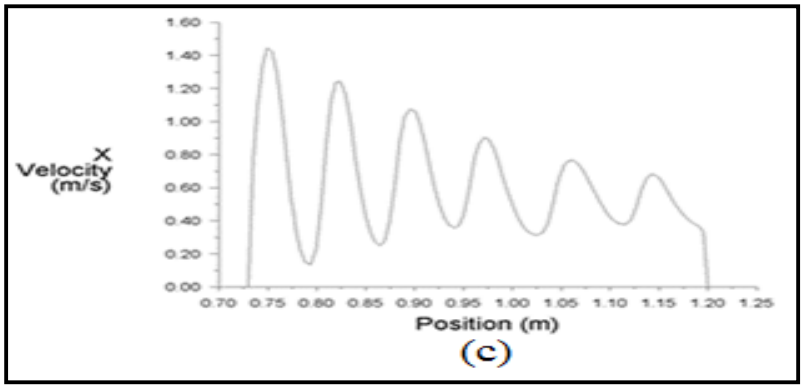

Figure No.8: Horizontal velocity profile against Z-axis at spallation region for rounded target with (a) 3 (b) 4 and (c) 5 vanes. (Notice that the number of troughs in graph are equal to the number of vanes)

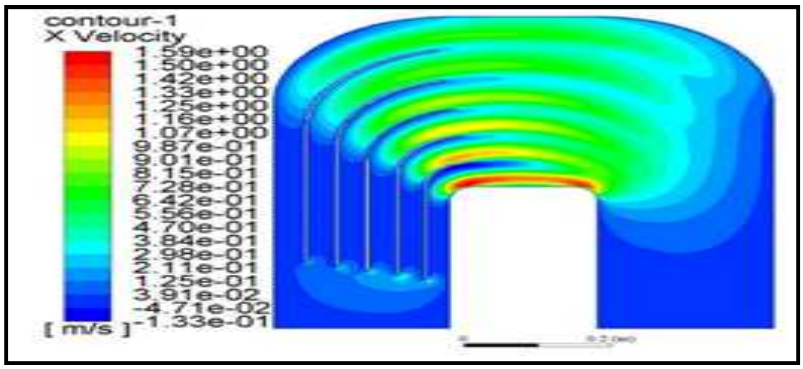

Figure No.9: x-velocity component in modified inverted-U target with 5 vanes

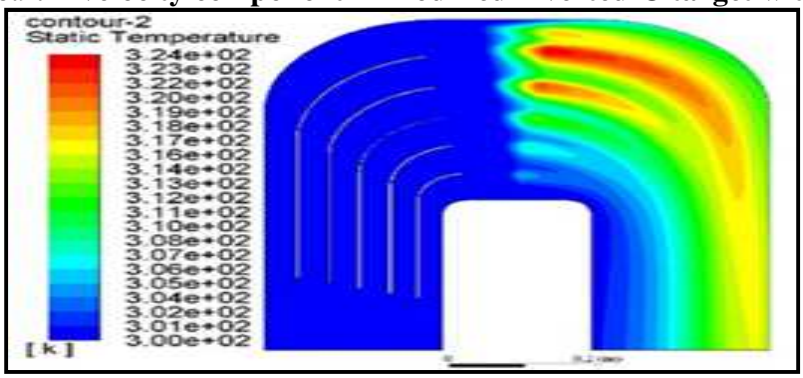

Figure No.10: Steady temperature contours in modified inverted-U design with 5 vanes at heat flux of 500MW/m

CONCLUSION

Numerical fluid flow and heat transfer simulation was done with suitable models for two different types of ADS target geometries with finite volume CFD code Fluent. It was seen that the inverted-U design had a more stable interface than falling liquid metal jet design like MYRRHA. Basic inverted-U design can be modified to include guide vanes and rounded edges which eliminate recirculation zones. Vanes also guide the flow till the interface to achieve high velocity that is needed to advect the heat generated by spallation.

ACKNOWLEDGEMENT

The authors wish to express their sincere gratitude to Department of Mechanical Engineering, PSG College of Technology, Coimbatore, Tamil Nadu, India for providing necessary facilities to carry out this research work.

CONFLICT OF INTEREST

We declare that we have no conflict of interest.

BIBLIOGRAPHY

1. Rubbia, C, Rubio J A, Buono S, Carminati F, Fietier N, Galvez J, Geles C, Kadi Y, Klapisch R, Mandrillon P, Revol J P and Roche Ch. Conceptual design of a fast neutron operated high power energy amplifier, *CERN Report, CERN-AT-95-44 (ET), Geneva,* 1995, 187-312.
2. Arul Prakash K, Biswas G and Rathish Kumar B V. Thermal hydraulics of the spallation target module of an accelerator driven sub-critical system: A numerical study, *International Journal of Heat and Mass Transfer,* 49(23-24), 2006, 4633-4652.
3. Cho C, Kim Y, Song T Y and Lee Y. Numerical design of a 20MW lead-bismuth spallation target with an injection tube, *Nuc Eng and Desi,* 238(1), 2008, 90-101.
4. Roelofs F, de Jager B, Class A, Jeanmart H, Schuurmans P, Ciampichetti A, Gerbeth G, Stieglitz R, Fazio C. European research on HLM thermal-hydraulics for ADS applications, *Jou of Nuc Mat,* 376(3), 2008, 401-404.

5. http://myrrha.sckcen.be/en
6. Class A. G, Angeli D, Batta A, Dierckx M, Fellmoser F. XT-ADS Windowless spallation target thermohydraulic design and experimental setup, *Journal of Nuclear Materials,* 415(3), 2011, 378-384.
7. Su G. Y, Gu H. Y, Cheng X. Experimental and numerical studies on free surface flow of windowless target, *Annals of Nuclear Energy,* 43(1), 2012, 142-149.
8. Liu J, Gao l, Yang l *et al*. Effect of adding a swirl on flow pattern and recirculation zone in ADS windowless spallation target, *Nuclear Engineering Design,* 276, 2014, 249-258.
9. Zhenqin Xiong, Hanyang Gu, Shenjie Gong. Experimental and numerical study on the flow pattern of the ADS windowless spallation target with a second free surface downstream using model fluid water, *Nuclear Engineering Design,* 279, 2015, 179-187.
10. Jeanmart H, Bricteux L, Tichelen K, Dierckx M. Characterisation in water experiments of a detached flow free surface spallation target, *Journal of Nuclear Material,* 415(3), 2011, 385-395.
11. Litfin K, Batta A, Class A G *et al*. Experimental and numerical investigation of liquid-metal free-surface flows in spallation targets, *Nuclear Engineering and Design,* 290, 2015, 107-118.
12. Bianchi F, Ferri R and Moreau V. Thermo-hydraulic analysis of the windowless target system, *Nuclear Engineering Design,* 238(8), 2008, 2135-2145.
13. Hirt C W, Nichols B D. Volume of fluid (VOF) method for the dynamics of free boundaries, *Journal of Computational Physics,* 39(1), 1981, 201-225.
14. ANSYS Fluent-solver theory guide, release 16.1, *Canonsburg (PA): ANSYS Inc,* 2015, 1-814.
15. Sobolev V. Thermophysical properties of lead and lead–bismuth eutectic, *Journal of Nuclear Material,* 362(2-3), 2007, 235-247.
16. Brackbill J U, Kothe D B and Zemach C. A continuum method for modelling surface tension, *Journal of Computational Physics,* 100(2), 1992, 335-354.
17. Young D. L. Time dependent multi-material flow with large fluid distortion, Numerical Methods for Fluid Dynamics (book chapter), *Edit by K. W. Montes and M. J. Baines, Academic Press, New York, USA,* 1982, 273-285.
18. Liu J, Gao L, Tong J F *et al*. Study of steady-state heat transfer with various large beam intensities in ADS windowless spallation target, *Applied Thermal Engineering,* 88(9), 2015, 444-445.

Please cite this article in press as: Senthil Kumar A P *et al*. CFD Analysis of flow in windowless accelerated driven sub-critical (ADS) reactor target module, *International Journal of Engineering and Robot Technology,* 7(2), 2020, 55-64.